Available online at www.sciencedirect.com
SCIENCE DIRECT®
International Journal of Solids and Structures 41 (2004) 6647–6660
INTERNATIONAL JOURNAL OF SOLIDS and STRUCTURES
www.elsevier.com/locate/ijsolstr

Compression stiffness of infinite-strip bearings of laminated elastic material interleaving with flexible reinforcements

Hsiang-Chuan Tsai *

Department of Construction Engineering, National Taiwan University of Science and Technology, P.O. Box 90-130, Taipei 106, Taiwan

Received 29 May 2004
Available online 20 July 2004

Abstract

The closed-form solutions to the compression stiffness of the laminated elastomeric bearings of infinite-strip shape with flexible reinforcements are derived. The effect of bulk compressibility in the elastic layer and the effect of boundary condition at the ends of the bearing are considered. Three types of the elastic layers bonded to flexible reinforcements are studied. The first type simulates the interior elastic layers of the bearings with shear-free ends. The second type simulates the exterior elastic layers of the free-end bearings. The third type simulates the elastic layers in the bearings which ends are bonded to rigid plates. The theoretical solutions to the compression stiffness of the bearings are extremely close to the results obtained by the finite element method, which proves that the displacement assumptions utilized in the theoretical derivation are reasonable.

Keywords: Bonded elastic layer; Elastomeric bearing; Seismic isolation

1. Introduction

A laminated elastomeric bearing consists of elastomeric layers bonded to interleaving reinforcing sheets. High stiffness of reinforcements restrains the lateral expansion of elastomeric layers and results in higher compression stiffness than an unbonded elastomeric layer in the vertical direction normal to the layer. Thus, a laminated elastomeric bearing can provide high vertical rigidity to sustain gravity loading, while still providing the same horizontal flexibility of an unbonded elastomer.

The laminated rubber bearings used in seismic isolation are heavy and expensive. The primary weight in an isolation bearing is due to the reinforcing steel plates. The high cost of producing an isolator results from the labor involved in preparing the steel plates and assembly of the rubber sheets and steel plates for vulcanization bonding in a mold. The research work performed by Kelly (1999) suggests that eliminating

* Tel.: +886-2-27376581; fax: +886-2-27376606.
E-mail address: hctsai@mail.ntust.edu.tw (H.-C. Tsai).

0020-7683/$ - see front matter © 2004 Elsevier Ltd. All rights reserved.
doi:10.1016/j.ijsolstr.2004.06.005

the steel reinforcing plates and replacing them with fiber reinforcement can significantly reduce both the weight and the cost of isolators. The reduction in weight is possible because fiber materials are now available with an elastic stiffness that is of the same as steel. Manufacturing cost may be reduced because the use of fiber allows a simpler, less labor-intensive process.

To analyze the stiffness of the steel-reinforced bearing, the steel reinforcement is treated as completely rigid and the bonded elastic layer deforms according to two kinematics assumptions: (i) planes parallel to the rigid bonding plates before deformation remain planar after loading; (ii) lines normal to the rigid bonding plates before deformation become parabolic after loading. Gent and Lindley (1959) derived the compression stiffness of an incompressible elastic layer bonded to rigid plates for infinite-strip shape and circular shape. Subsequently, Gent and Meinecke (1970) extended this method to analyze the compression stiffness and tilting stiffness of incompressible elastic layers for square and other shapes.

Although rubber can be treated as incompressible in some analyses, the assumption of incompressibility tends to overestimate the stiffness of the bonded rubber layer when the layer's shape factor (defined as the ratio of the one bonded area to the force-free area) is high. Kelly (1997) developed a 'pressure solution' approach to derive the compression stiffness and the tilting stiffness considering the effect of bulk compressibility. The solutions are available for the layers of infinite-strip shape (Chaihoub and Kelly, 1991), circular shape (Chaihoub and Kelly, 1990) and square shape (Koh and Kelly, 1987).

Lindley (1979a) applied an energy method to derive the compression stiffness of the infinite-strip and circular shapes as well as the tilting stiffness of the infinite-strip shape (Lindley, 1979b) for the material of any Poisson's ratio. Koh and Kelly (1989) utilized a 'variable transform' approach to derive the compression stiffness of the square shape for compressible material. Recently, Koh and Lim (2001) extended this approach to solve the compression stiffness of the rectangular shape. Tsai and Lee (1998, 1999) developed a pressure approach to derive the compression stiffness and tilting stiffness of bonded elastic layers in infinite-strip, circular and square shapes. These solutions are accurate for the material of any Poisson's ratio.

In contrast to the steel reinforcement that is assumed to be rigid, the fiber reinforcement is flexible in extension. Tsai and Kelly (2001, 2002a,b) derived the compression stiffness and tilting stiffness of fiber-reinforced isolators by assuming the elastomeric layer is incompressible and the reinforcement is flexible. Recently, bulk compressibility is included in the stiffness analysis of fiber-reinforced isolators of infinite-strip shape (Kelly, 2002; Kelly and Takhirov, 2002). In these researches, the flexible reinforcements in the bearing are assumed to have the same deformation, which implies every elastic layer in the bearing has the same compression stiffness and is referred to as 'monotonic deformation' here.

In the bearing with rigid reinforcements, each bonded elastic layer has the same compression stiffness because of rigid reinforcement. However, this may not be applicable to the bearings with flexible reinforcement, where the compression stiffness of bonded elastic layers varies with the deformation of flexible reinforcements. Moreover, the boundary condition at the ends of the fiber-reinforced bearings can also affect the compression stiffness. When performing the compression analysis of the bearing subjected to vertical loading only, two types of boundary conditions can be imposed at the ends of the bearing, which are referred to as 'free end' and 'rigid end' here. 'Free end' means the end of the bearing does not have any horizontal constraint so that it is free from any shear force. 'Rigid end' means the end of the bearing is bonded to rigid plate so that it does not have any horizontal deformation.

In this paper, the effect of bulk compressibility in the elastic layer and the effect of boundary condition at the ends of the bearing are considered in the compression analysis of fiber-reinforced bearings. A theoretical approach similar to the analysis by Tsai and Lee (1998) is developed to derive the compression stiffness of fiber-reinforced bearings of infinite-strip shape. The stiffness of the bearing with monotonic deformation is derived first. Then, the free-end bearings and the rigid-end bearings are studied. In addition to the theoretical derivation, finite element analyses on the fiber-reinforced bearings are carried out to verify the exactness of the theoretical solution.

2. Governing equations

A bearing of infinite-strip shape shown in Fig. 1 consists of multiple elastic layers interleaving with flexible reinforcing sheets. The elastic layer 1 is at the top of the bearing and the elastic layer n is at the bottom. The reinforcements are counted from 0 to n. The width of the bearing is $2b$ and each elastic layer has the same thickness t. The length of the bearing is much larger than the other dimensions, so that the deformation of the bearing is assumed to be in plane strain state and only a unit length of the bearing is analyzed. Fig. 2 depicts the elastic layer i bonded between the reinforcements $i-1$ and i. A local coordinate system (x, y, z) is located at the center of the layer. The y-axis is attached to the infinite-long direction.

For isotropic elastic layers, the mean pressure p has the following relation with the displacements

$$p(x,z) = -\kappa(u_{,x} + w_{,z}) \tag{1}$$

where u and w are the displacements of the elastic layer along the x and z directions, respectively, κ is the bulk modulus, and the commas imply differentiation with respect to the indicated coordinate. The normal stresses in the x and z directions have the forms

$$\sigma_{xx} = -\frac{\lambda}{\kappa}p + 2\mu u_{,x} \tag{2}$$

$$\sigma_{zz} = -\frac{\lambda}{\kappa}p + 2\mu w_{,z} \tag{3}$$

in which λ and μ are Lame's constants. The equilibrium equation in the x direction becomes

$$\frac{p_{,x}}{\kappa} = \frac{\mu}{\lambda + 2\mu}(u_{,zz} - w_{,xz}) \tag{4}$$

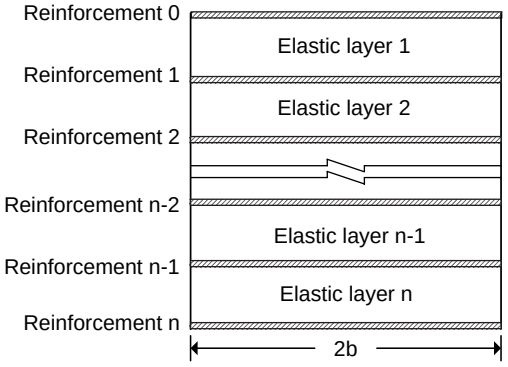

Fig. 1. Bearing consisting of n elastic layers interleaving with reinforcements.

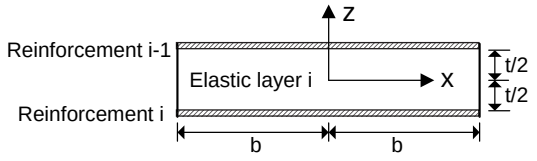

Fig. 2. Coordinate system in elastic layer.

The thickness of the reinforcements t_f is much smaller than the thickness of the elastic layers, so that the stress in the reinforcements can be regarded as being in plane stress state within x–y plane. Let N_{xx} be the normal force in the x direction acting on a unit length of the reinforcement, and u_f be the displacement of the reinforcement in the x direction, which have the following relation

$$N_{xx}(x) = \frac{E_f t_f}{1 - v_f^2} u_{f,x}(x) \tag{5}$$

where E_f and v_f are the elastic modulus and Poisson's ratio of the reinforcement, respectively.

When the bearing is subjected to vertical compression, horizontal planes of the bearing are assumed to remain plane, which implied that the vertical displacement of the elastic layer is a function of z only,

$$w(x,z) = \bar{w}(z) \tag{6}$$

The effective compression strain of the elastic layer ε_c is defined as

$$\varepsilon_c = -\frac{1}{t}[\bar{w}(t/2) - \bar{w}(-t/2)] \tag{7}$$

The compression stiffness of an elastic layer is determined by the effective compression modulus defined as

$$E_c = -\frac{1}{\varepsilon_c}\left\{\frac{1}{2b}\int_{-b}^{b}\left[\frac{1}{t}\int_{-t/2}^{t/2}\sigma_{zz}(x,z)\mathrm{d}z\right]\mathrm{d}x\right\} \tag{8}$$

Using Eq. (3), the effective compression modulus becomes

$$E_c = 2\mu + \frac{\lambda}{2b\varepsilon_c\kappa}\int_{-b}^{b}\bar{p}\,\mathrm{d}x \tag{9}$$

with $\bar{p}$ being the effective pressure defined as

$$\bar{p}(x) = \frac{1}{t}\int_{-t/2}^{t/2} p(x,z)\mathrm{d}z \tag{10}$$

The boundary condition of normal stress at the edge of the elastic layer is $\sigma_{xx}(b,z) = 0$. Substitute Eq. (2) into this boundary condition and then integrating through the thickness of the layer, which gives

$$\frac{\bar{p}(b)}{\kappa} = \frac{2\mu}{\lambda t}\int_{-t/2}^{t/2} u_{,x}(b,z)\mathrm{d}z \tag{11}$$

The boundary condition of the normal force at the edge of the reinforcing sheet is $N_{xx}(b) = 0$. From Eq. (5), this boundary condition means

$$u_{f,x}(b) = 0 \tag{12}$$

3. Bearings with monotonic deformation

The bearing with monotonic deformation assumes that all reinforcements have the same horizontal displacement, which allows the horizontal displacement of the elastic layers to have the form

$$u(x,z) = \bar{u}(x)\left(1 - \frac{4z^2}{t^2}\right) + u_f(x) \tag{13}$$

in which the term of $\bar{u}$ represents the kinematics assumption of quadratic-varied displacement. Substituting the displacement functions in Eqs. (6) and (13) into Eq. (1), the effective pressure defined in Eq. (10) becomes

$$\frac{\bar{p}}{\kappa} = -\left(\frac{2}{3}\bar{u}_{,x} + u_{\mathrm{f},x} - \varepsilon_{\mathrm{c}}\right) \tag{14}$$

Integrated through the thickness of the elastic layer, the equilibrium equation in Eq. (4) becomes

$$\frac{\bar{p}_{,x}}{\kappa} = -\frac{2}{3}\alpha_0^2\bar{u} \tag{15}$$

with

$$\alpha_0 = \frac{1}{t}\sqrt{\frac{12\mu}{\lambda + 2\mu}} \tag{16}$$

Using Eq. (15), Eq. (14) gives

$$u_{\mathrm{f},x} = \frac{1}{\alpha_0^2}\frac{\bar{p}_{,xx}}{\kappa} - \frac{\bar{p}}{\kappa} + \varepsilon_{\mathrm{c}} \tag{17}$$

The internal forces acing on the reinforcement are shown in Fig. 3, which gives the following equilibrium equation

$$\frac{\mathrm{d}N_{xx}}{\mathrm{d}x} + \tau_{xz}(x, -t/2) - \tau_{xz}(x, t/2) = 0 \tag{18}$$

where $\tau_{xz}(x, -t/2)$ and $\tau_{xz}(x, t/2)$ are the bonding shear stresses generated by the elastic layers bonded to the top and bottom, respectively, of the reinforcement. Under the assumption of monotonic deformation, the shear stress in each elastic layer has the same form

$$\tau_{xz}(x, z) = -\mu\frac{8z}{t^2}\bar{u}(x) \tag{19}$$

Substituting Eqs. (5) and (19) into Eq. (18), the equilibrium equation in the reinforcement becomes

$$u_{\mathrm{f},xx} = -\frac{2}{3}\alpha_1^2\bar{u} \tag{20}$$

with

$$\alpha_1 = \sqrt{\frac{12\mu(1 - \nu_{\mathrm{f}}^2)}{E_{\mathrm{f}}t_{\mathrm{f}}t}} \tag{21}$$

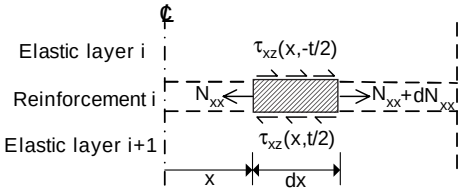

Fig. 3. Internal forces acting on reinforcement.

From Eq. (15), Eq. (20) becomes

$$u_{\mathrm{f},xx} = \frac{\alpha_1^2}{\alpha_0^2}\bar{p}_{,x} \tag{22}$$

Substitution of Eq. (17) into Eq. (22) yields

$$\frac{\bar{p}_{,xxx}}{\kappa} - (\alpha_0^2 + \alpha_1^2)\frac{\bar{p}_{,x}}{\kappa} = 0 \tag{23}$$

Using Eqs. (13) and (14), the boundary condition in Eq. (11) becomes

$$\frac{\bar{p}(b)}{\kappa} = \frac{2\mu}{\lambda + 2\mu}\varepsilon_{\mathrm{c}} \tag{24}$$

According to Eqs. (17) and (24), the boundary condition in Eq. (12) means

$$\frac{\bar{p}_{,xx}(b)}{\kappa} = -\frac{\lambda}{\lambda + 2\mu}\alpha_0^2\varepsilon_{\mathrm{c}} \tag{25}$$

Based on the above two boundary conditions and the fact that $\bar{p}(x)$ is an even function, the solution of Eq. (23) is

$$\frac{\bar{p}(x)}{\kappa} = \varepsilon_{\mathrm{c}}\left[\frac{2\mu}{\lambda + 2\mu} + \frac{\lambda}{\lambda + 2\mu}\left(\frac{\alpha_0^2}{\beta_0^2}\right)\left(1 - \frac{\cosh\beta_0 x}{\cosh\beta_0 b}\right)\right] \tag{26}$$

with

$$\beta_0 = \sqrt{\alpha_0^2 + \alpha_1^2} \tag{27}$$

Substituting Eq. (26) into Eq. (9), the effective compression modulus of the elastic layer in the bearing with monotonic deformation is

$$(E_{\mathrm{c}})_{\mathrm{mono}} = 2\mu + \frac{2\mu\lambda}{\lambda + 2\mu} + \frac{\lambda^2}{\lambda + 2\mu}\left(\frac{\alpha_0^2}{\beta_0^2}\right)\left(1 - \frac{\tanh\beta_0 b}{\beta_0 b}\right) \tag{28}$$

As $\lambda = \infty$, the asymptotic value is

$$(E_{\mathrm{c}})_{\mathrm{mono}} = 4\mu + \frac{12\mu}{\alpha_1^2 t^2}\left(1 - \frac{\tanh\alpha_1 b}{\alpha_1 b}\right) \tag{29}$$

which is the compression modulus of the elastic layer of incompressible material. The last term is the same as the solution derived by Kelly (1999). The asymptotic value of Eq. (28) for $E_{\mathrm{f}} = \infty$ is

$$E_{\mathrm{c}} = 2\mu + \lambda\left(1 - \frac{\lambda}{\lambda + 2\mu}\frac{\tanh\alpha_0 b}{\alpha_0 b}\right) \tag{30}$$

which is the compression modulus of the elastic layer bonded between rigid plates (Tsai and Lee, 1998).

Substitution of Eq. (26) into Eq. (22) gives the displacement of reinforcement

$$u_{\mathrm{f}} = \varepsilon_{\mathrm{c}} b\left(\frac{\lambda}{\lambda + 2\mu}\right)\left(\frac{\alpha_1^2}{\beta_0^2}\right)\left[\frac{x}{b} - \left(\frac{1}{\beta_0 b}\right)\frac{\sinh\beta_0 x}{\cosh\beta_0 b}\right] \tag{31}$$

Using Eq. (5), the normal force in the reinforcement is found as

$$N_{xx} = \varepsilon_{\mathrm{c}}\left(\frac{\lambda}{\lambda + 2\mu}\right)\left(\frac{12\mu}{\beta_0^2 t}\right)\left(1 - \frac{\cosh\beta_0 x}{\cosh\beta_0 b}\right) \tag{32}$$

As $E_f = \infty$, the asymptotic value is

$$N_{xx} = \varepsilon_c t\lambda\left(1 - \frac{\cosh \alpha_0 x}{\cosh \alpha_0 b}\right) \tag{33}$$

which is the distribution of the normal force in the rigid reinforcement.

4. Bearings with free ends

When analyzing the free-end bearing where both ends are free from any horizontal shear force, the elastic layers can be distinguished into two groups, exterior and interior. The exterior layers are the elastic layers at the top and the bottom of the bearing. The interior layers are the other elastic layers. In the elastic layer 1, one of the exterior layers, the horizontal displacement can be assumed as

$$u^{(1)}(x,z) = \bar{u}^{(1)}(x)\left(1 - \frac{4z^2}{t^2}\right) + u_f^{(0)}(x)\left(\frac{1}{2} + \frac{z}{t}\right) + u_f^{(1)}(x)\left(\frac{1}{2} - \frac{z}{t}\right) \tag{34}$$

in which $u_f^{(i)}$ represents the displacement of the reinforcement i. Substituting the above equation and Eq. (6) into Eq. (1), the effective pressure defined in Eq. (10) becomes

$$\frac{\bar{p}^{(1)}}{\kappa} = -\left(\frac{2}{3}\bar{u}_{,x}^{(1)} + \frac{1}{2}u_{f,x}^{(0)} + \frac{1}{2}u_{f,x}^{(1)} - \varepsilon_c^{(1)}\right) \tag{35}$$

where $\varepsilon_c^{(1)}$ is the effective compression strain of the elastic layer 1 defined in Eq. (7).

Integrated through the thickness of the elastic layer, the equilibrium equation in Eq. (4) for the elastic layer 1 becomes

$$\frac{\bar{p}_{,x}^{(1)}}{\kappa} = -\frac{2}{3}\alpha_0^2\bar{u}^{(1)} \tag{36}$$

Using Eq. (36), Eq. (35) becomes

$$u_{f,x}^{(0)} + u_{f,x}^{(1)} = 2\left(\frac{1}{\alpha_0^2}\frac{\bar{p}_{,xx}^{(1)}}{\kappa} - \frac{\bar{p}^{(1)}}{\kappa} + \varepsilon_c^{(1)}\right) \tag{37}$$

The top of the reinforcement 0 is free from shear force, so that its equilibrium equation becomes

$$\frac{dN_{xx}^{(0)}}{dx} - \tau_{xz}^{(1)}(x, t/2) = 0 \tag{38}$$

where $\tau_{xz}^{(1)}$ is the bonding shear force applied by the elastic layer 1 at the bottom of the reinforcement. By using Eqs. (5) and (34), the above equation becomes

$$u_{f,xx}^{(0)} = \frac{1}{12}\alpha_1^2(-4\bar{u}^{(1)} + u_f^{(0)} - u_f^{(1)}) \tag{39}$$

The equilibrium equation of the reinforcing sheet 1 is

$$\frac{dN_{xx}^{(1)}}{dx} + \tau_{xz}^{(1)}(x, -t/2) - \tau_{xz}^{(2)}(x, t/2) = 0 \tag{40}$$

By assuming the horizontal displacement of the elastic layer 2 be monotonically deformed as shown in Eq. (13), the above equilibrium equation becomes

$$u_{\mathrm{f},xx}^{(1)} = \frac{1}{12}\alpha_1^2(-4\bar{u}^{(1)} - 4\bar{u}^{(2)} - u_{\mathrm{f}}^{(0)} + u_{\mathrm{f}}^{(1)}) \tag{41}$$

Since the elastic layers 1 and 2 are adjacent, it is reasonable to assume these two elastic layers have the same bulge deformations, i.e.

$$\bar{u}^{(2)}(x) \approx \bar{u}^{(1)}(x) \tag{42}$$

Summation of Eqs. (39) and (41) yields

$$u_{\mathrm{f},xx}^{(0)} + u_{\mathrm{f},xx}^{(1)} = -\alpha_1^2\bar{u}^{(1)} \tag{43}$$

Substitution of Eqs. (36) and (37) into Eq. (43) gives

$$\frac{\bar{p}_{,xxx}^{(1)}}{\kappa} - \left(\alpha_0^2 + \frac{3}{4}\alpha_1^2\right)\frac{\bar{p}_{,x}^{(1)}}{\kappa} = 0 \tag{44}$$

Using Eqs. (34) and (35), the boundary condition in Eq. (11) becomes

$$\frac{\bar{p}^{(1)}(b)}{\kappa} = \frac{2\mu}{\lambda + 2\mu}\varepsilon_{\mathrm{c}}^{(1)} \tag{45}$$

From Eq. (12),

$$u_{\mathrm{f},x}^{(0)}(b) + u_{\mathrm{f},x}^{(1)}(b) = 0 \tag{46}$$

Substitute Eq. (37) into the above equation and use Eq. (45), which leads another boundary condition of the effective pressure

$$\frac{\bar{p}_{,xx}^{(1)}(b)}{\kappa} = -\frac{\lambda}{\lambda + 2\mu}\alpha_0^2\varepsilon_{\mathrm{c}}^{(1)} \tag{47}$$

Using the above two boundary conditions and the fact that $\bar{p}^{(1)}(x)$ is an even function, the solution of Eq. (44) is

$$\frac{\bar{p}^{(1)}(x)}{\kappa} = \varepsilon_{\mathrm{c}}^{(1)}\left[\frac{2\mu}{\lambda + 2\mu} + \frac{\lambda}{\lambda + 2\mu}\left(\frac{\alpha_0^2}{\beta_1^2}\right)\left(1 - \frac{\cosh\beta_1 x}{\cosh\beta_1 b}\right)\right] \tag{48}$$

with

$$\beta_1 = \sqrt{\alpha_0^2 + 0.75\alpha_1^2} \tag{49}$$

Substituting Eq. (48) into Eq. (9), the effective compression modulus of the elastic layer 1 at the top of the free-end bearing is derived as

$$E_{\mathrm{c}}^{(1)} = 2\mu + \frac{2\mu\lambda}{\lambda + 2\mu} + \frac{\lambda^2}{\lambda + 2\mu}\left(\frac{\alpha_0^2}{\beta_1^2}\right)\left(1 - \frac{\tanh\beta_1 b}{\beta_1 b}\right) \tag{50}$$

As $\lambda = \infty$, the asymptotic value is

$$E_{\mathrm{c}}^{(1)} = 4\mu + \frac{12\mu}{0.75\alpha_1^2 t^2}\left(1 - \frac{\tanh\sqrt{0.75}\alpha_1 b}{\sqrt{0.75}\alpha_1 b}\right) \tag{51}$$

The elastic layer n at the bottom of the free-end bearing has the same effective compression modulus as shown in Eq. (50). The interior layers are assumed to be monotonically deformed and have the effective

compression modulus shown in Eq. (28). The stiffness of the bearing can be obtained by adding the stiffness of the elastic layers in series. The effective compression modulus of the free-end bearing having n elastic layers is

$$(E_c)_{free} = \frac{n}{\frac{2}{E_c^{(1)}} + \frac{n-2}{(E_c)_{mono}}} \tag{52}$$

The shape factor of the bonded elastic layer of infinite-strip shape is defined as

$$S = \frac{b}{t} \tag{53}$$

Let E and v be the elastic modulus and Poisson's ratio of the elastic layer, respectively. The ratio of the elastic layer stiffness to the reinforcement stiffness γ is defined as

$$\gamma = \frac{Et(1-v_f^2)}{E_f t_f} \tag{54}$$

Eqs. (28) and (50) indicate that the normalized effective compression modulus E_c/E is a function of v, S and γ.

Fig. 4 compares the effective compression modulus among Eq. (28) for interior elastic layers, Eq. (50) for exterior elastic layers, and Eq. (52) for the free-end bearing consisting of five elastic layers. The results of finite element analysis for the five-layer bearing are also plotted in the figure. The stiffness of exterior layers is higher than the stiffness of interior layers. The effective compression modulus calculated from Eq. (52) is the closest curve to the finite element solution. Eqs. (27) and (49) indicates that the stiffness difference between the exterior layer and the interior layer becomes negligible when the stiffness ratio γ is very small. When the bearing has a large number of elastic layers, Eq. (52) indicates that $(E_c)_{free}$ becomes close to $(E_c)_{mono}$.

Variations of the effective compression modulus with Poisson's ratio v and stiffness ratio γ are plotted in Figs. 5 and 6, respectively, for the free-end bearings consisting of 20 elastic layers, which show that the theoretical solutions calculated from Eq. (52) are very close to the finite element solutions. The bearing with higher shape factor has a higher stiffness. The bearing stiffness increases with increasing Poisson's ratio v. The bearing with high shape factor ($S = 20$) and high reinforcement stiffness ($\gamma = 0.01$) has a dramatic increase in stiffness when Poisson's ratio v is near 0.5. The bearing stiffness decreases with decreasing the

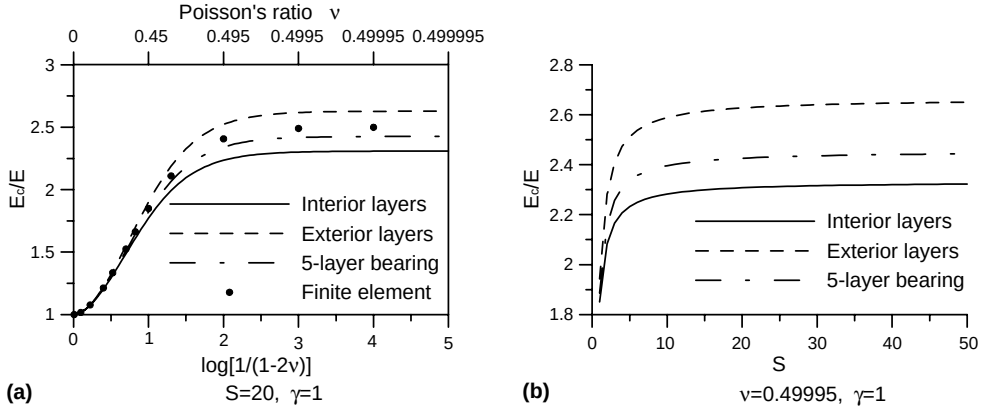

Fig. 4. Effective compression modulus of exterior layers and interior layers.

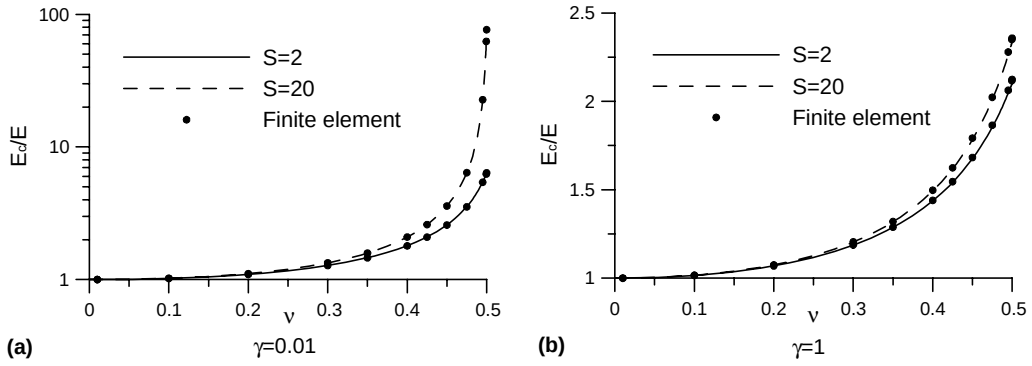

Fig. 5. Effective compression modulus varied with Poisson's ratio in 20-layer bearing with free ends.

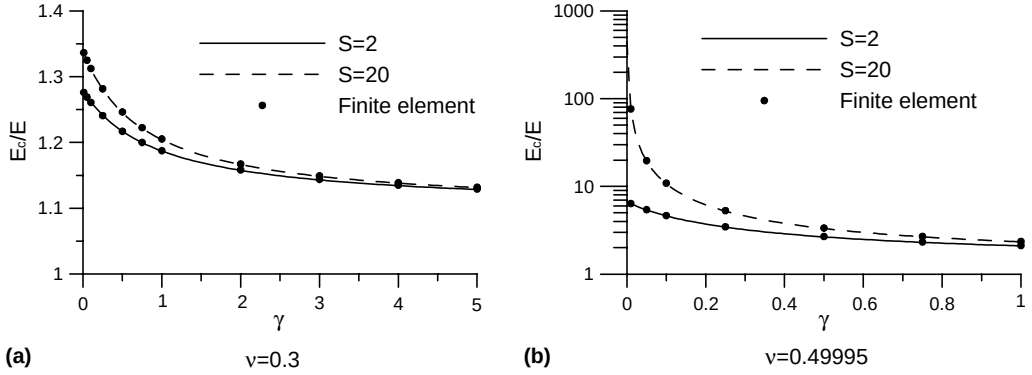

Fig. 6. Effective compression modulus varied with stiffness ratio in 20-layer bearing with free ends.

reinforcement stiffness (increasing γ). When $\gamma \to \infty$, the free-end bearing becomes an unbonded elastic block and its effective compression modulus becomes $E/(1-\nu^2)$ which is independent of the shape factor S.

5. Bearings with rigid ends

For the bearing with rigid ends, the reinforcements at the ends of the bearings are subjected to rigid constraint, i.e. $u_{\mathrm{f}}^{(0)}(x) = u_{\mathrm{f}}^{(n)}(x) = 0$. When deriving the compression stiffness of the elastic layer i in the rigid-end bearing, the horizontal displacements of the reinforcements $i-1$, i and $i+1$ are assumed to be proportional to a displacement function $\tilde{u}^{(i)}(x)$, that is

$$u_{\mathrm{f}}^{(i-1)}(x) = f_{i-1}\tilde{u}^{(i)}(x), \quad u_{\mathrm{f}}^{(i)}(x) = f_i\tilde{u}^{(i)}(x), \quad u_{\mathrm{f}}^{(i+1)}(x) = f_{i+1}\tilde{u}^{(i)}(x) \tag{55}$$

where f_i is a dimensionless quadratic function varied through the height of the bearing. For the bearing consisting of n elastic layers, f_i has the following form

$$f_i = 4\frac{i}{n}\left(1 - \frac{i}{n}\right) \tag{56}$$

The horizontal displacement of the elastic layer i in the bearing can be assumed as

$$u^{(i)}(x,z) = \bar{u}^{(i)}(x)\left(1 - \frac{4z^2}{t^2}\right) + u_{\mathrm{f}}^{(i-1)}(x)\left(\frac{1}{2} + \frac{z}{t}\right) + u_{\mathrm{f}}^{(i)}(x)\left(\frac{1}{2} - \frac{z}{t}\right) \tag{57}$$

The vertical displacement of the elastic layer has the same form as Eq. (6). Substituting Eqs. (6) and (57) into Eq. (1), the effective pressure of the elastic layer i defined in Eq. (10) becomes

$$\frac{\bar{p}^{(i)}}{\kappa} = -\left[\frac{2}{3}\bar{u}_{,x}^{(i)} + \frac{1}{2}(f_{i-1} + f_i)\tilde{u}_{,x}^{(i)} - \varepsilon_{\mathrm{c}}^{(i)}\right] \tag{58}$$

where $\varepsilon_{\mathrm{c}}^{(i)}$ is the effective compression strain of the elastic layer i defined in Eq. (7).

Integrated through the thickness of the elastic layer, the equilibrium equation in Eq. (4) becomes

$$\frac{\bar{p}_{,x}^{(i)}}{\kappa} = -\frac{2}{3}\alpha_0^2\bar{u}^{(i)} \tag{59}$$

Using Eq. (59), Eq. (58) becomes

$$\tilde{u}_{,x}^{(i)} = \frac{2}{f_i + f_{i-1}}\left(\frac{1}{\alpha_0^2}\frac{\bar{p}_{,xx}^{(i)}}{\kappa} - \frac{\bar{p}^{(i)}}{\kappa} + \varepsilon_{\mathrm{c}}^{(i)}\right) \tag{60}$$

The equilibrium equation of the reinforcement i is

$$\frac{\mathrm{d}N_{xx}^{(i)}}{\mathrm{d}x} + \tau_{xz}^{(i)}(x,-t/2) - \tau_{xz}^{(i+1)}(x,t/2) = 0 \tag{61}$$

where $\tau_{xz}^{(i)}$ is the shear stress in the elastic layer i with the form, from Eq. (57),

$$\tau_{xz}^{(i)}(x,z) = \frac{\mu}{t}\left[\bar{u}^{(i)}(x)\left(-8\frac{z}{t}\right) + u_{\mathrm{f}}^{(i-1)}(x) - u_{\mathrm{f}}^{(i)}(x)\right] \tag{62}$$

Substitute Eqs. (5) and (62) into Eq. (61) and use the assumptions in Eq. (55) and $\bar{u}^{(i+1)}(x) \approx \bar{u}^{(i)}(x)$, which gives

$$\tilde{u}_{,xx}^{(i)} = \frac{\alpha_1^2}{12f_i}[-8\bar{u}^{(i)} + (-f_{i+1} + 2f_i - f_{i-1})\tilde{u}^{(i)}] \tag{63}$$

Differentiate Eqs. (59) and (63) with respect to x and then combine the results and Eq. (60), which yields

$$\frac{\bar{p}_{,xxxx}^{(i)}}{\kappa} - (\alpha_0^2 + \alpha_{2i}^2 + \alpha_{3i}^2)\frac{\bar{p}_{,xx}^{(i)}}{\kappa} + \alpha_0^2\alpha_{2i}^2\frac{\bar{p}^{(i)}}{\kappa} = \alpha_0^2\alpha_{2i}^2\varepsilon_{\mathrm{c}}^{(i)} \tag{64}$$

with

$$\alpha_{2i}^2 = \frac{\alpha_1^2(-f_{i+1} + 2f_i - f_{i-1})}{12f_i} = \frac{2\alpha_1^2}{3n^2f_i} \tag{65}$$

$$\alpha_{3i}^2 = \frac{\alpha_1^2(f_i + f_{i-1})}{2f_i} \tag{66}$$

Using Eqs. (57) and (58), the boundary condition in Eq. (11) becomes

$$\frac{\bar{p}^{(i)}(b)}{\kappa} = \frac{2\mu}{\lambda + 2\mu}\varepsilon_{\mathrm{c}}^{(i)} \tag{67}$$

Substituting Eqs. (55) and (60) into Eq. (12) and using Eq. (67) lead another boundary condition of the effective pressure

$$\frac{\bar{p}^{(i)}_{,xx}(b)}{\kappa} = -\frac{\lambda}{\lambda+2\mu}\alpha_0^2\varepsilon_c^{(i)} \tag{68}$$

Using the above two boundary conditions and the fact that $\bar{p}^{(i)}(x)$ is an even function, the solution of Eq. (64) is

$$\frac{\bar{p}^{(i)}(x)}{\kappa} = \varepsilon_c^{(i)}\left\{1-\frac{\lambda}{\lambda+2\mu}\left[\left(\frac{\beta_{3i}^2-\alpha_0^2}{\beta_{3i}^2-\beta_{2i}^2}\right)\frac{\cosh\beta_{2i}x}{\cosh\beta_{2i}b}+\left(\frac{\beta_{2i}^2-\alpha_0^2}{\beta_{2i}^2-\beta_{3i}^2}\right)\frac{\cosh\beta_{3i}x}{\cosh\beta_{3i}b}\right]\right\} \tag{69}$$

with

$$\beta_{2i}^2 = \frac{1}{2}\left[\alpha_0^2+\alpha_{2i}^2+\alpha_{3i}^2-\sqrt{(\alpha_0^2+\alpha_{2i}^2+\alpha_{3i}^2)^2-4\alpha_0^2\alpha_{2i}^2}\right] \tag{70}$$

$$\beta_{3i}^2 = \frac{1}{2}\left[\alpha_0^2+\alpha_{2i}^2+\alpha_{3i}^2+\sqrt{(\alpha_0^2+\alpha_{2i}^2+\alpha_{3i}^2)^2-4\alpha_0^2\alpha_{2i}^2}\right] \tag{71}$$

Substituting Eq. (69) into Eq. (9), the effective compression modulus of the elastic layer i is derived as

$$E_c^{(i)} = 2\mu+\lambda\left\{1-\frac{\lambda}{\lambda+2\mu}\left[\left(\frac{\beta_{3i}^2-\alpha_0^2}{\beta_{3i}^2-\beta_{2i}^2}\right)\frac{\tanh\beta_{2i}b}{\beta_{2i}b}+\left(\frac{\beta_{2i}^2-\alpha_0^2}{\beta_{2i}^2-\beta_{3i}^2}\right)\frac{\tanh\beta_{3i}b}{\beta_{3i}b}\right]\right\} \tag{72}$$

As $\lambda=\infty$, the asymptotic value is

$$E_c^{(i)} = 4\mu+\frac{4\mu}{(\alpha_{2i}^2+\alpha_{3i}^2)t^2}\left[\alpha_{2i}^2b^2+\frac{3\alpha_{3i}^2}{(\alpha_{2i}^2+\alpha_{3i}^2)}\left(1-\frac{\tanh\sqrt{(\alpha_{2i}^2+\alpha_{3i}^2)}b}{\sqrt{(\alpha_{2i}^2+\alpha_{3i}^2)}b}\right)\right] \tag{73}$$

Adding the stiffness of each elastic layer in series can create the effective compression modulus of the rigid-end bearing consisting of n elastic layers as

$$(E_c)_{\text{rigid}} = \frac{n}{\sum_{i=1}^{n}\frac{1}{E_c^{(i)}}} \tag{74}$$

It should be noted that the formula of $E_c^{(i)}$ in Eq. (72) is not suitable for $E_c^{(n)}$, because Eq. (61) requires that the elastic layer $i+1$ have to exist below the reinforcement i. However, due to the symmetry of the loading, the stiffness of the bottom elastic layer is the same as that of the top elastic layer, i.e. $E_c^{(n)} = E_c^{(1)}$.

Variations of the effective compression modulus with Poisson's ratio v and stiffness ratio γ are plotted in Figs. 7 and 8, respectively, for the rigid-end bearings consisting of 20 elastic layers, which show that the theoretical solutions calculated from Eq. (74) are very close to the finite element solutions. When the reinforcement stiffness is high ($\gamma=0.01$), the stiffness of the rigid-end bearing is very close to the stiffness of the free-end bearing. When the reinforcement stiffness is low ($\gamma=1$), the stiffness of the rigid-end bearing is higher than the stiffness of the free-end bearing because of the rigid constraint at the ends of the bearing. When $\gamma\to\infty$, the rigid-end bearing becomes an elastic block bonded by the rigid plates at the ends of the bearing and its effective compression modulus is dependent on the shape factor S and the number of elastic layers.

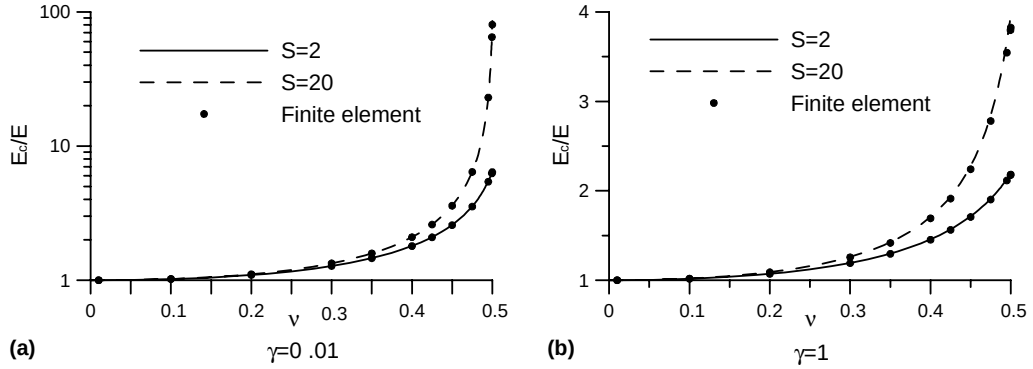

Fig. 7. Effective compression modulus varied with Poisson's ratio in 20-layer bearing with rigid ends.

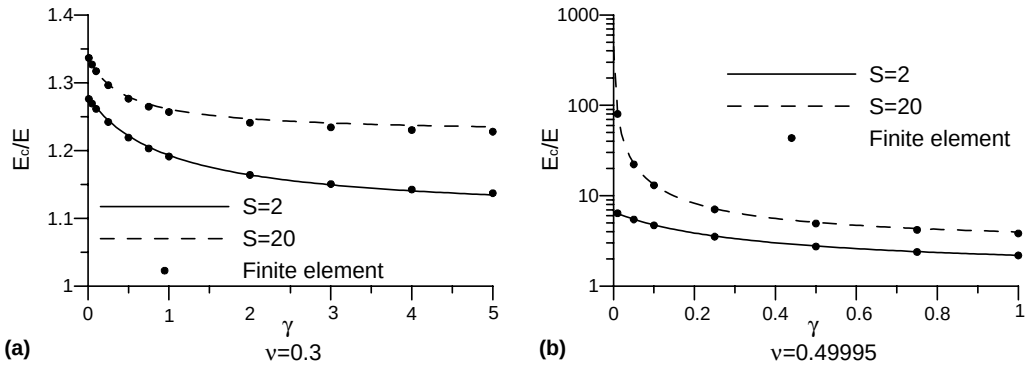

Fig. 8. Effective compression modulus varied with stiffness ratio in 20-layer bearing with rigid ends.

6. Conclusion

The closed-form solutions of compression stiffness for the elastic layers bonded between flexible reinforcements in the infinite-strip bearings are derived. Three types of bonded elastic layers are studied. The first type assumes that every elastic layer in the bearing has the same deformation, which simulates the interior elastic layers of the bearings with shear-free ends. The second type simulates the exterior elastic layers of the free-end bearings where one side of the top reinforcement is free from shear force when the bearing is subjected to the compression force. Combining the stiffness of exterior layers and the stiffness of interior layers in series can generate the compression stiffness of the free-end bearings. When the numbers of elastic layers in the bearing is large, the stiffness contribution of the exterior layers to the bearing becomes less significant, and the effective compression modulus of the bearing becomes close to that of the interior layer. The third type simulates the elastic layers in the bearings which ends are bonded to rigid plates. The effective compression modulus of the rigid-end bearing is higher than that of the free-end bearing. When the stiffness of the reinforcement is high, the effective compression modulus of the rigid-end bearing is close to that of the free-end bearing. The compression stiffness of the bearings calculated from the theoretical solution is extremely close to the result obtained from the finite element method, which proves that the displacement assumptions utilized in the theoretical derivation are reasonable. Because the compressibility

effect of the elastic layer is considered in theoretical derivation, the closed-form solutions are accurate for the elastic layers of any Poisson's ratio.

Acknowledgements

The National Science Council of Taiwan supported the research work reported in this paper under Grant no. NSC91-2211-E011-015. This support is greatly appreciated.

References

Chaihoub, M.S., Kelly, J.M., 1990. Effect of bulk compressibility on the stiffness of cylindrical base isolation bearings. International Journal of Solids and Structures 26, 734–760.

Chaihoub, M.S., Kelly, J.M., 1991. Analysis of infinite-strip shaped base isolator with elastomer bulk compression. Journal of Engineering Mechanics, ASCE 117, 1791–1805.

Gent, A.N., Lindley, P.B., 1959. The compression of bonded rubber block. Proceeding of the Institution Mechanical Engineers 173, 111–117.

Gent, A.N., Meinecke, E.A., 1970. Compression, bending and shear of bonded rubber blocks. Polymer Engineering and Science 10, 48–53.

Kelly, J.M., 1997. Earthquake-Resistant Design with Rubber, second ed. Springer-Verlag, London.

Kelly, J.M., 1999. Analysis of fiber-reinforced elastomeric isolator. Journal of Seismology and Earthquake Engineering 2, 19–34.

Kelly, J.M., 2002. Seismic isolation systems for developing countries. Earthquake Spectra 18, 385–406.

Kelly, J.M., Takhirov, S.M., 2002. Analytical and experimental study of fiber-reinforced strip isolators. PEER Report 2002/11, Pacific Earthquake Engineering Research Center, University of California, Berkeley.

Koh, C.G., Kelly, J.M., 1987. Effects of axial load on elastomeric isolation bearings. Report UCB/EERC-86/12, Earthquake Engineering Research Center, University of California, Berkeley.

Koh, C.G., Kelly, J.M., 1989. Compression stiffness of bonded square layers of nearly incompressible material. Engineering Structures 11, 9–15.

Koh, C.G., Lim, H.L., 2001. Analytical solution for compression stiffness of bonded rectangular layers. International Journal of Solids and Structures 38, 445–455.

Lindley, P.B., 1979a. Compression module for blocks of soft elastic material bonded to rigid end plates. Journal of Strain Analysis 14, 11–16.

Lindley, P.B., 1979b. Plane strain rotation module for blocks of soft elastic blocks. Journal of Strain Analysis 14, 17–21.

Tsai, H.-C., Kelly, J.M., 2001. Stiffness analysis of fiber-reinforced elastomeric isolators. PEER Report 2001/05, Pacific Earthquake Engineering Research Center, University of California, Berkeley.

Tsai, H.-C., Kelly, J.M., 2002a. Stiffness analysis of fiber-reinforced rectangular seismic isolators. Journal of Engineering Mechanics, ASCE 128, 462–470.

Tsai, H.-C., Kelly, J.M., 2002b. Bending stiffness of fiber-reinforced circular seismic isolators. Journal of Engineering Mechanics, ASCE 128, 1150–1157.

Tsai, H.-C., Lee, C.-C., 1998. Compressive stiffness of elastic layers bonded between rigid plates. International Journal of Solids and Structures 35, 3053–3069.

Tsai, H.-C., Lee, C.-C., 1999. Tilting stiffness of elastic layers bonded between rigid plates. International Journal of Solids and Structures 36, 2485–2505.